Voxel seed coherent source analysis on transient global amnesia patients*

Muthuraman M, Döhring J, Nahrwold M, Mideksa KG, Chaitanya CV, Margraf N, Raethjen J, Deuschl G, Bartsch T.

Abstract— **Transient global amnesia (TGA) is a rare neurological disorder with a sudden, temporary episode of memory loss which usually occurs in old age. The episodic loss of memory becomes normal after a stipulated time of approximately 24 hours. The precise pathology is not yet completely understood. Moreover, there is no proper neuroimaging method to assess this condition. In this study, the EEG was measured at two time points one with the occurrence of the episode (acute) and the second time point after the patient returns to the normal memory condition (follow-up). The aim of the study was to look at the pathological network involved during the acute phase and the follow up phase in these patients for the five frequency bands, namely, delta, theta, alpha, beta, and gamma. The method used for the source analyses was a beamforming approach called dynamic imaging of coherent sources in the frequency domain. The seed voxel was the lesion area taken from the anatomical MRI of each patient. The cortical and sub-cortical network comprised of the caudate and cerebellum in case of the delta band frequency. Two temporal sources in case of the theta band. Temporal, medial frontal, parietal, putamen, and thalamus sources were found in case of the alpha band. Prefrontal, parietal, and thalamus sources were found in case of the beta band. Temporal and thalamus in case of the gamma band frequency. All these sources were involved in the acute phase. Moreover, in the follow-up phase the motor area, in all frequency bands except gamma band, was additionally active followed by parietal and occipital regions in alpha and gamma frequencies. The differences involved in the network of sources between the two phases gives us better understanding of this neurological disorder.**

I. Introduction

The underlying pathophysiology is not very clear for the transient global amnesia (TGA) patients [1]. TGA is depicted by a short hyper-acute phase in which the memory is severely affected and after 24 hours the patients gradually recover their memory [2, 3]. The neuroimaging modalities which were used so far to disentangle this disease are positron emission tomography (PET) [4, 5], functional magnetic resonance imaging (fMRI) [6, 7], and diffusion weighted imaging (DWI) [8, 9]. The modality EEG has been used in assessing the TGA patients during acute and follow-up phases and has showed differences in the five frequency bands [10, 11]. However, all the studies have concentrated on the scalp level analysis and not on the source level in order to analyze the networks involved. The coherent source analysis approach has shown that EEG is capable of detecting the oscillatory network of sources in the five frequency bands [12]. The network of sources involved can help us in better understanding of the pathophysiology behind this neurological disorder. To detect the coherent network of sources involved in these patients we first found the lesion Montreal Neurological Institute (MNI) co-ordinates from each patient. Then we used the lesion as the seed voxel for finding out the network of sources coupled with it during the acute and follow-up phase. In this way we know exactly the network responsible for the pathophysiology instead a more explorative approach of looking at the whole brain for strong active sources at each of the frequency bands. In the present study, we identified all the network of sources involved in both phases for the five frequency bands, which could help in building an easy neuroimaging tool to assess this rare neurological disorder.

*Research supported by SFB 855 Project D2.

M. Muthuraman., J. Döhring, N. Margraf, J. Raethjen, G. Deuschl, T. Bartsch are with the Department of Neurology, Christian Albrecht's university Kiel, 24105 Germany m.muthuraman@neurologie.uni-kiel.de, j.döhring@neurologie.uni-kiel.de, n.margraf@neurologie.uni-kiel.de, j.raethjen@neurologie.uni-kiel.de, g.deuschl@neurologie.uni-kiel.de, t.bartsch@neurologie.uni-kiel.de.

M. Nahrwold, KG. Mideksa and CV Chaitanya are with the Institute for Digital Signal Processing and System Theory, Faculty of Engineering, Christian Albrecht's university Kiel, 24143 Germany MartinNahrwold@web.de kgm@tf.uni-kiel.de, venkatachaitanya409@gmail.com.

II. Methods

A. Data acquisition

In this study twelve female and five male transient global amnesia patients participated. The study was acknowledged by the local ethics committee, University of Kiel, Germany and the patients gave their informed consent. In these patients, eight of them had left sided lesion, six of them right sided lesion, and three of them had bi-lateral lesions. The mean age of the patients was 67.76±5.41 years. The MNI co-ordinates of the lesion for each patient were identified form the structural anatomical MRI. The whole brain MRI's of the patients were performed 24-72 hours after the onset of TGA symptoms where the detectability of hippocampal lesions is the highest. High-resolution MRI's were performed on a 3 T unit (Philips Intera Achieva) as reported in the previous study [13]. All the lesions were mirrored to the right hemisphere so totally there were 20 lesions from 17 patients. The mean MNI co-ordinates from the patients were they had

left sided lesion were [-32.72±-1.48; -20.27±-7.12; -17±-4.89 mm]. Similarly, the mean MNI-co-ordinates for the patients with the right sided lesion were [30.67±-2.5; -21.55±-6.50; -14.22±-5.89 mm]. The patients were seated in a comfortable chair in a slightly reclined position. Both forearms were supported by firm arm rests up to the wrist joints. The subjects were asked to keep their eyes open and fix it at a point located 2 m away. The EEG was recorded with a standard 10-20 system with 21-channels using a unipolar Fpz reference electrode. The EEG was sampled at 500 Hz and band-pass filtered (0.05-200 Hz). In addition to the EEG electrodes, an EOG electrode was placed below the eye lid in order to correct for the eye-artefacts in the raw data. Each patient had two recording sessions: during the acute TGA episode, named, *acute*, and the follow-up recording, named, *control* 12 months (±9 months SD) after the episode when the patients were completely recovered and when the CA1 lesion was resolved [9].

B. Realistic head models

The forward problem is the computation of the scalp potentials for a set of neural current sources. It is solved by estimating the lead-field matrix with specified models for the head. In this study, the head was modeled using individual MRI's to create realistic head models. Figure 1 shows the three layers which were modelled for one of the representative patient's that will be used by the boundary element method to solve the forward problem. The open-source software "Fieldtrip" was used [14]. In order to map the current dipoles in the human brain to the voltages on the scalp, the lead-field matrix (LFM) needs to be calculated. The LFM contains information about the geometry and conductivity of the model. The LFM was estimated based on the divergence of the source current density vector at each node, rather than three orthogonal current dipoles within each element. The node oriented basis is derived directly from the element stiffness matrix A, and the right-hand side vector S_n. It is straight forward to solve the well-conditioned system using equation (1)

$$\phi = A^{-1} S_n \tag{1}$$

to recover the potentials, ϕ, throughout the volume when the sources are known. For source analysis, however we are not interested in the electric field throughout the volume, but only in the fields at those few nodes corresponding to the scalp electrode recording sites. In this case, a matrix R is introduced to select those electrode potentials from ϕ. R is a $[K \times M]$ matrix. Each row of R contains a single non-zero entry: the value 1.0 located at the column corresponding to the node index for that electrode. From equation (1), we now select a subset of ϕ by applying R:

$$\phi_r = R\phi = RA^{-1} S_n \tag{2}$$

The RA^{-1} operator is a node-oriented lead-field basis, which we term L_n, and for it follow that:

$$L_n S_n = \phi_r \tag{3}$$

In order to efficiently compute RA^{-1}, we can exploit the sparse nature of R. Since R contains M non-zero entries, we only need to construct the corresponding M columns of A^{-1}. This is accomplished by solving equation (4)

$$A(A^{-1})_m = I_m \tag{4}$$

where $(A^{-1})_m$ is unknown for source m. In this way we are able to attain the LFM for the BEM model.

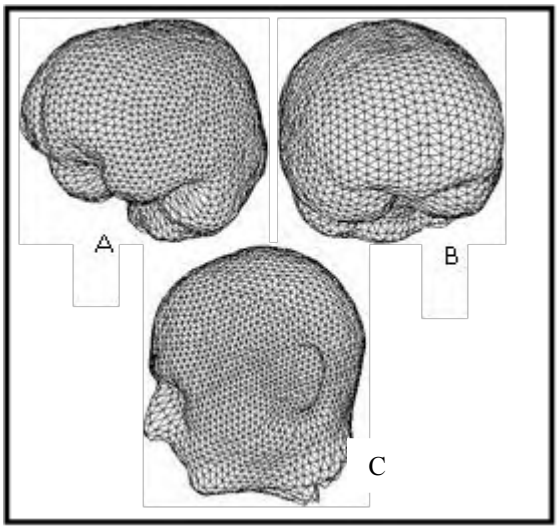

Figure 1. A. shows the realistic head model for the skull, B. for the brain C.for the skin modelled from one patient. The traingles are the mesh which are depicted on each of these three surfaces.

C. Source analysis

To localize the brain activity that is coherent with the reference (lesion) region, the dynamic imaging of coherent sources (DICS) method was used. DICS is efficient in localizing the coherent network of sources for a specific frequency band [12, 15]. The spatial filtering used in this algorithm gives the ability to do further analysis on the time series extracted from these source regions. The inverse problem is the quantitative estimation of the properties of the underlying neuronal current sources that produce the EEG signals. The neural activity is modeled as a current dipole or sum of current dipoles. The power and coherence at any given location in the brain can be computed using a linear transformation which, in our case, is the spatial filter. In this study, the linear constrained minimum variance (LCMV) spatial filter was used which relates the underlying neural activity to the electromagnetic field on the scalp surface. The main aim of the LCMV method is to design a bank of spatial filters that attenuates signals from other locations and permits signals generated from a particular location in the brain. The DICS method make use of this spatial filter algorithm to identify the spatial maximum power and coherence in the brain for a particular frequency band. In this study, the spatial extent of each voxel is defined to be 5mm.

We used a regularization value of $\alpha = 0.001$. This value is chosen due to the reason that it is tested, for not yielding spurious spatial extension of sources for a voxel definition of 5 mm, in simulations and successfully applied on real data. The same reference (lesion) region was used for the cortico-cortical coherence analysis of all the frequency bands. In order to create topographic maps, the spatial filter is applied to a large number of voxels covering the entire brain using a voxel size of 5 mm. The individual maps of coherence were spatially normalized and interpolated on an individual T1 brain images in SPM8. For each patient, the reference region was identified from the individual diffusion-weighted imaging MRI and the brain source coherent with the reference region was found for each individual band. In order to find the next strongest coherent source with the reference region, the first coherent source with the reference region was projected out of the coherence matrix, and further coherent areas were found. The statistical significance of the identified coherent sources was tested by a baseline analysis.

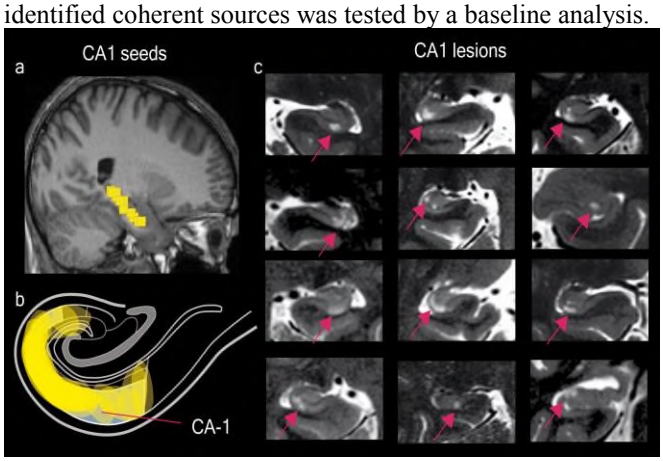

Figure 2. A) Shows the seeds used for the source analyses in a sagittal slice for all the 17 patients. B) Synopsis of all DWI/ TR2R lacunar lesions depicted from T2 weighted images of each patient and transferred to an anatomical template of the cornu ammonis. C) shows the CA1 lesions on a representative MR saggital slices.

The acute data from the first condition rest was taken as the baseline for analyzing the changes in the control data also during rest. At the end, the grand average from all the patients with the left, right, and bi-lateral lesions (two values were included in the average) network of sources for each frequency band is mirrored to the right side of the brain on a standard MRI.

III. Results

A. Coherent network of sources

The dynamic imaging of coherent sources (DICS) method was applied to the EEG data from the resting condition by taking the hippocampus lesion source signal as defined by the MNI co-ordinates for each patient in Table 1. The identified network of significant ($p = 0.005$) coherent sources for the corresponding frequencies are shown in Figure 2. The delta frequency band was associated with the sources in the sensory-motor cortex (source 1, BA4), caudate nuclei (source 2), and the cerebellum (source 3, BA 19). The theta frequency was associated with temporal gyrus (source 1, BA20), uncus (source 2, BA 36), and sensory-motor cortex (source3, BA4). For the alpha frequency, the network of sources were temporal gyrus (source 1, BA20), medial frontal cortex (source2, BA9), sensory-motor cortex (source3, BA4), parietal cortex (source 4, BA39), putamen (source 5), and thalamus (source 6, BA23). In the beta frequency, the sources were dorso lateral prefrontal cortex (source1, BA46), sensory-motor cortex (source2, BA4), parietal cortex (source 3, BA39), middle and lateral thalamus (source 4, BA23). The gamma frequency showed coherent sources at the temporal gyrus (source 1, BA20), occipital cortex (source 2, BA17), and the thalamus (source 3, BA23).

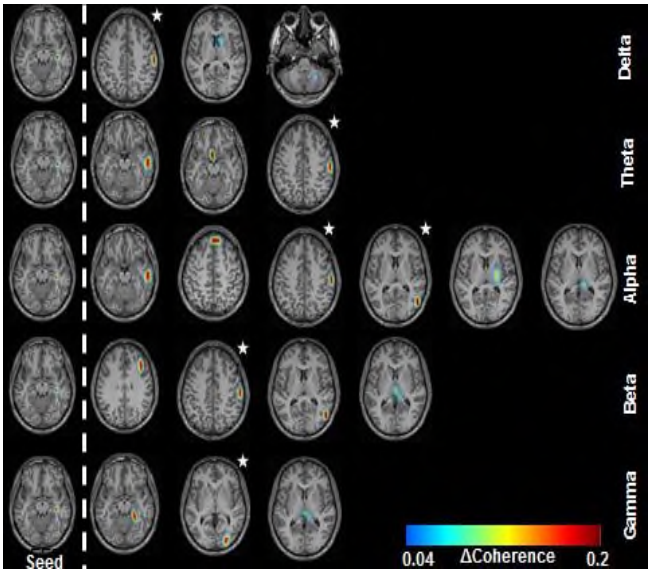

Figure 3. The grandaverage from all 17 patients. The first column indicates the seed voxel which was used for each freqeuency band. The rows show the network of sources invloved for each frequency band, respectively. The soures with white (*) indicate the additional source identifed for the control phase.The colorbar indicates the minimum and maximum coherence values for all the frequency bands. The Δcoherence shows the differnce between the acute and the control phase.

IV. Discussion

The EEG combined with the source analysis could be a useful tool for the better understanding of the networks involved in this neurological disorder. The earlier studies on PET [4, 16], task related fMRI studies [5, 6, 17], and resting state fMRI [7] have also demonstrated changes in the network of regions and not only in the hippocampus region. The results from this study also depict that hippocampus lesion is only a part of the network which is seen structurally in the MRI. Furthermore, the network of activation includes additional sources in the control phase which was not active during acute phase. In most of the studies the temporal and frontal sources have been discussed. From this study we could see that there is also sub-cortical involvement, like the caudate, putamen, thalamus, and cerebellum. Recently, it has

been hypothesized that the striatum, putamen, and basal ganglia are involved in the memory processes [18, 19]. All these evidences support our findings and prove that the EEG can effectively be used as an imaging tool for analyzing this group of patients.

In conclusion, the network re-adaptation for the complete recovery of these patients can be related to those additional sources in the control phase. In this way probably we will be able to develop a biomarker in the future for the acute and normal phase by looking at the network activations iof thes patients.

ACKNOWLEDGMENT

Support from the German Research Council (Deutsche Forschungsgemeinschaft, DFG, SFB 855, Project D2) is gratefully acknowledged.

REFERENCES

[1] M. Hainselin, P. Quinette, B. Desgranges, O. Martinaud, V. de La Sayette, D. Hannequin*, et al.*, "Awareness of disease state without explicit knowledge of memory failure in transient global amnesia," *Cortex,* vol. 48, pp. 1079-84, Sep 2012.

[2] P. Quinette, B. Guillery-Girard, J. Dayan, V. de la Sayette, S. Marquis, F. Viader*, et al.*, "What does transient global amnesia really mean? Review of the literature and thorough study of 142 cases," *Brain,* vol. 129, pp. 1640-58, Jul 2006.

[3] T. Bartsch and G. Deuschl, "Transient global amnesia: functional anatomy and clinical implications," *Lancet Neurol,* vol. 9, pp. 205-14, Feb 2010.

[4] J. C. Baron, M. C. Petit-Taboue, F. Le Doze, B. Desgranges, N. Ravenel, and G. Marchal, "Right frontal cortex hypometabolism in transient global amnesia. A PET study," *Brain,* vol. 117 (Pt 3), pp. 545-52, Jun 1994.

[5] F. Eustache, B. Desgranges, M. C. Petit-Taboue, V. de la Sayette, V. Piot, C. Sable*, et al.*, "Transient global amnesia: implicit/explicit memory dissociation and PET assessment of brain perfusion and oxygen metabolism in the acute stage," *J Neurol Neurosurg Psychiatry,* vol. 63, pp. 357-67, Sep 1997.

[6] R. Westmacott, F. L. Silver, and M. P. McAndrews, "Understanding medial temporal activation in memory tasks: evidence from fMRI of encoding and recognition in a case of transient global amnesia," *Hippocampus,* vol. 18, pp. 317-25, 2008.

[7] M. Peer, M. Nitzan, I. Goldberg, J. Katz, J. M. Gomori, T. Ben-Hur*, et al.*, "Reversible functional connectivity disturbances during transient global amnesia," *Ann Neurol,* vol. 75, pp. 634-43, May 2014.

[8] O. Sedlaczek, J. G. Hirsch, E. Grips, C. N. Peters, A. Gass, J. Wohrle*, et al.*, "Detection of delayed focal MR changes in the lateral hippocampus in transient global amnesia," *Neurology,* vol. 62, pp. 2165-70, Jun 22 2004.

[9] T. Bartsch, K. Alfke, R. Stingele, A. Rohr, S. Freitag-Wolf, O. Jansen*, et al.*, "Selective affection of hippocampal CA-1 neurons in patients with transient global amnesia without long-term sequelae," *Brain,* vol. 129, pp. 2874-84, Nov 2006.

[10] Y. H. Park, H. Y. Jeong, J. W. Jang, S. Y. Park, J. S. Lim, J. Y. Kim*, et al.*, "Disruption of the Posterior Medial Network during the Acute Stage of Transient Global Amnesia: A Preliminary Study," *Clin EEG Neurosci,* Nov 11 2014.

[11] Y. Kwon, Y. Yang, J. W. Jang, Y. H. Park, J. Kim, S. H. Park*, et al.*, "Left dominance of EEG abnormalities in patients with transient global amnesia," *Seizure,* vol. 23, pp. 825-9, Nov 2014.

[12] L. Michels, M. Muthuraman, R. Luchinger, E. Martin, A. R. Anwar, J. Raethjen*, et al.*, "Developmental changes of functional and directed resting-state connectivities associated with neuronal oscillations in EEG," *Neuroimage,* vol. 81, pp. 231-42, Nov 1 2013.

[13] T. Bartsch, K. Alfke, G. Deuschl, and O. Jansen, "Evolution of hippocampal CA-1 diffusion lesions in transient global amnesia," *Ann Neurol,* vol. 62, pp. 475-80, Nov 2007.

[14] R. Oostenveld, P. Fries, E. Maris, and J.-M. Schoffelen, "FieldTrip: Open Source Software for Advanced Analysis of MEG, EEG, and Invasive Electrophysiological Data," *Computational Intelligence and Neuroscience,* vol. 2011, 2011.

[15] J. Kujala, J. Gross, and R. Salmelin, "Localization of correlated network activity at the cortical level with MEG," *Neuroimage,* vol. 39, pp. 1706-20, Feb 15 2008.

[16] B. Guillery, B. Desgranges, V. de la Sayette, B. Landeau, F. Eustache, and J. C. Baron, "Transient global amnesia: concomitant episodic memory and positron emission tomography assessment in two additional patients," *Neurosci Lett,* vol. 325, pp. 62-6, May 31 2002.

[17] K. S. LaBar, D. R. Gitelman, T. B. Parrish, and M. M. Mesulam, "Functional changes in temporal lobe activity during transient global amnesia," *Neurology,* vol. 58, pp. 638-41, Feb 26 2002.

[18] S. Helie, S. W. Ell, and F. G. Ashby, "Learning robust cortico-cortical associations with the basal ganglia: An integrative review," *Cortex,* vol. 64C, pp. 123-135, Mar 2015.

[19] A. T. Mattfeld and C. E. Stark, "Functional contributions and interactions between the human hippocampus and subregions of the striatum during arbitrary associative learning and memory," *Hippocampus,* Jan 5 2015.